Supplemental Material for

Sequence determinants of allosteric back-to-front control of the Arf nucleotide switch

Noam Hantman[1], Tejaswi Koduru[2], Edgar V. Peters[3], Michel W. Jaworek[4], Scott A. McCallum[5], Richard E. Gillian[6], Roland Winter[4], Jacqueline Cherfils[7*], Catherine A. Royer[2*]

[1] Graduate Program in Biochemistry and Biophysics, Rensselaer Polytechnic Institute, Troy, NY 12180
[2] Department of Biological Sciences, Rensselaer Polytechnic Institute, Troy, NY 12180
[3] Department of Chemistry and Chemical Biology, Rensselaer Polytechnic Institute, Troy, NY 12180
[4] Department of Chemistry and Chemical Biology, Biophysical Chemistry, TU Dortmund University, D-44227 Dortmund, Germany
[5] Shirley Ann Jackson, PhD. Center for Biotechnology and Interdisciplinary Science, Rensselaer Polytechnic Institute, Troy, NY 12180
[6] Cornell High Energy Synchrotron Source, Cornell University, Ithaca, NY 14853
[7] Université Paris-Saclay, Ecole Normale Supérieure Paris-Saclay, CNRS, 91190 Gif-sur-Yvette, France

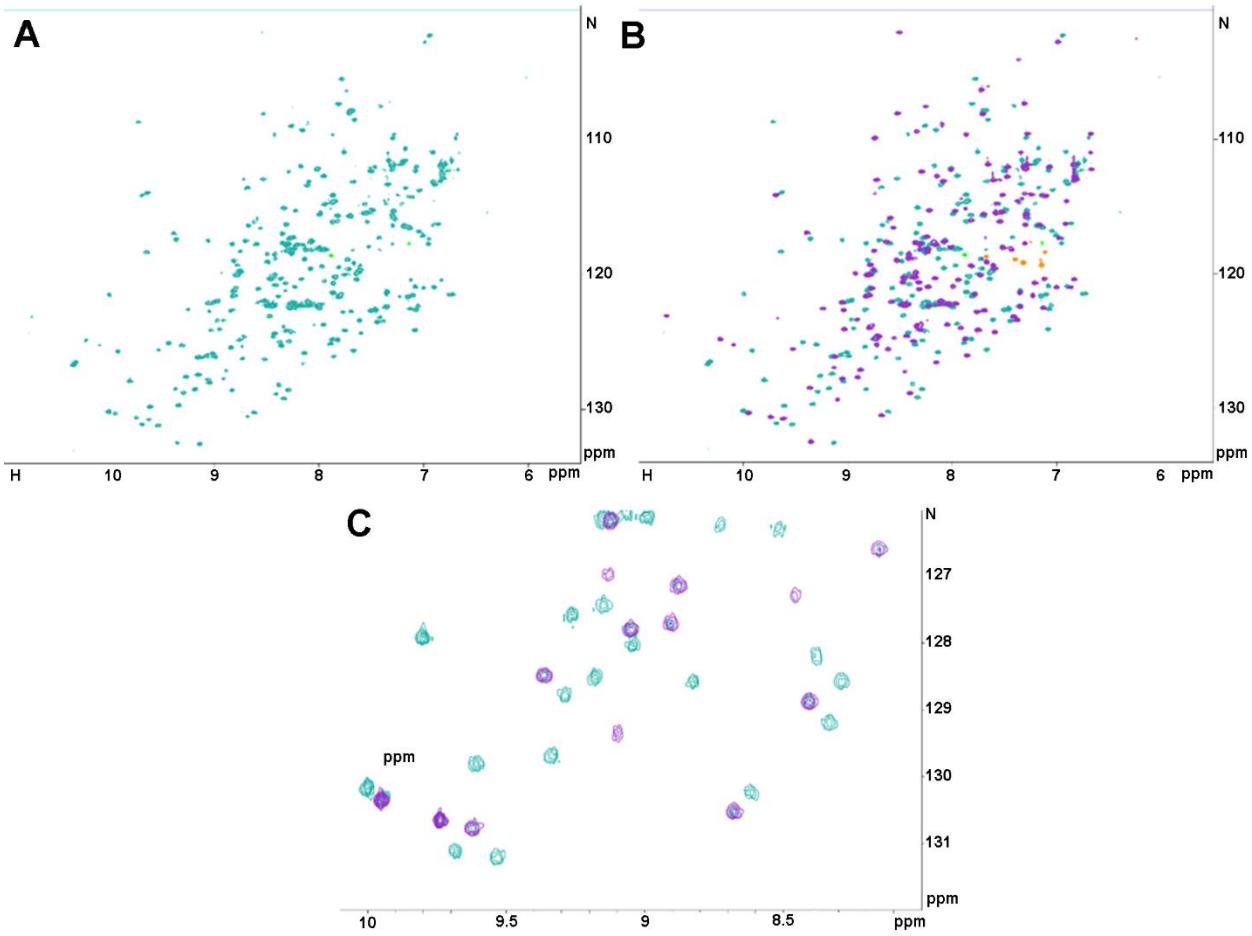

Figure S1. NMR spectra show Arf6 in a combination of multiple nucleotide-bound states. A) A 15N-1H HSQC of Arf6 without nucleotide loading. Several additional peaks are evident, most of which appear as a pair of peaks near to each other. B) An overlay of the spectrum before (green) and after (purple) loading with GDP. Many peaks present in the initial spectrum disappear, suggesting that the green spectrum represents Arf6 in multiple nucleotide-bound states. Peaks in orange and cyan represent aliased peaks. C) A zoomed-in region of B, clearly showing the reduction of two sets of peaks to one.

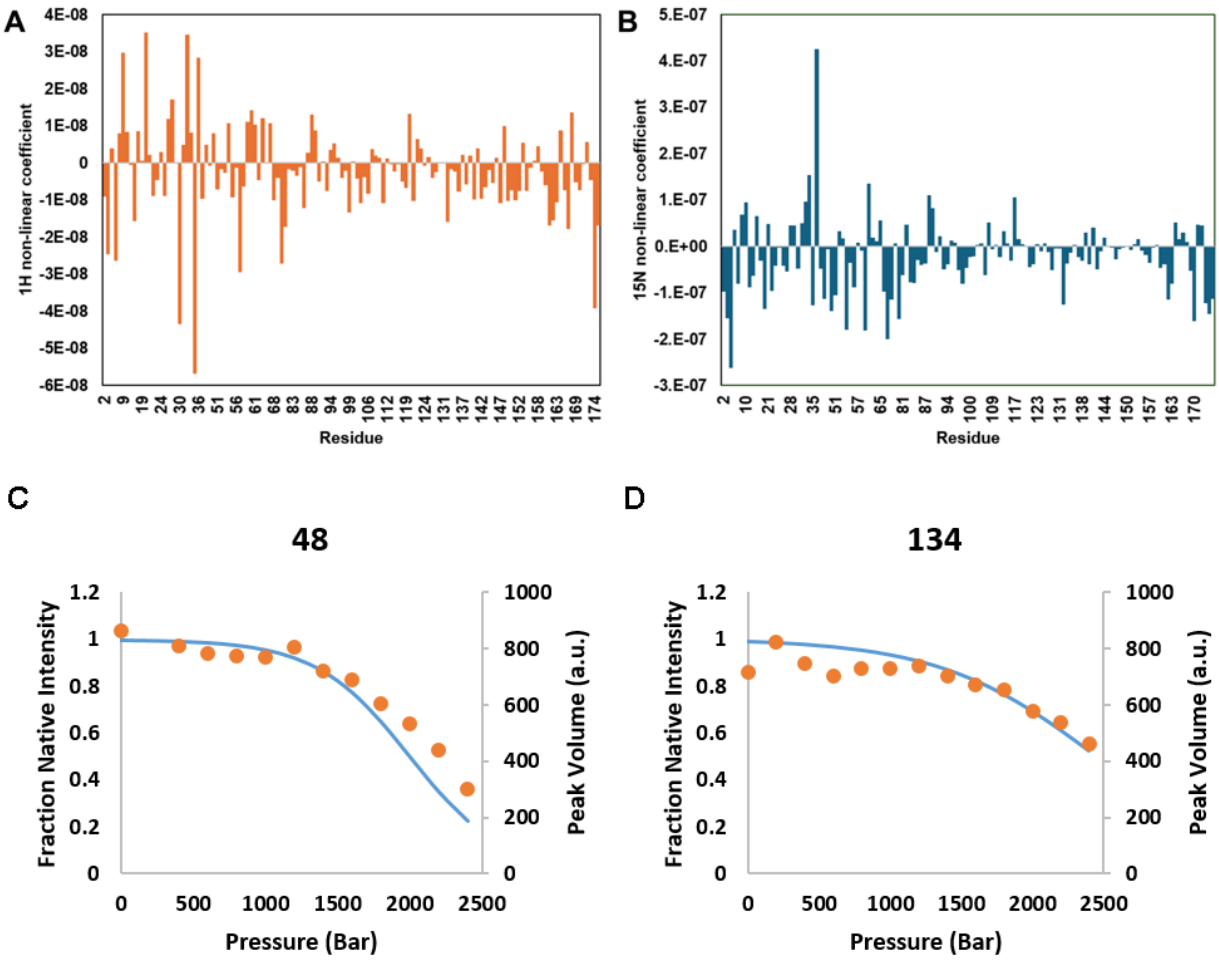

Figure S2. Pressure effects on non-Linear coefficients of chemical shift perturbations and peak volumes. A). The largest non-linear coefficients for both proton (left) and nitrogen (right) chemical shifts tend to be clustered in the switch regions, indicative of the existence of excited state populations. B) Examples of fit data based on NMR peak intensities (blue line) and measured peak volumes (orange points). Volumes decrease concomitantly with intensities, suggesting intensity loss is not due to peak broadening.

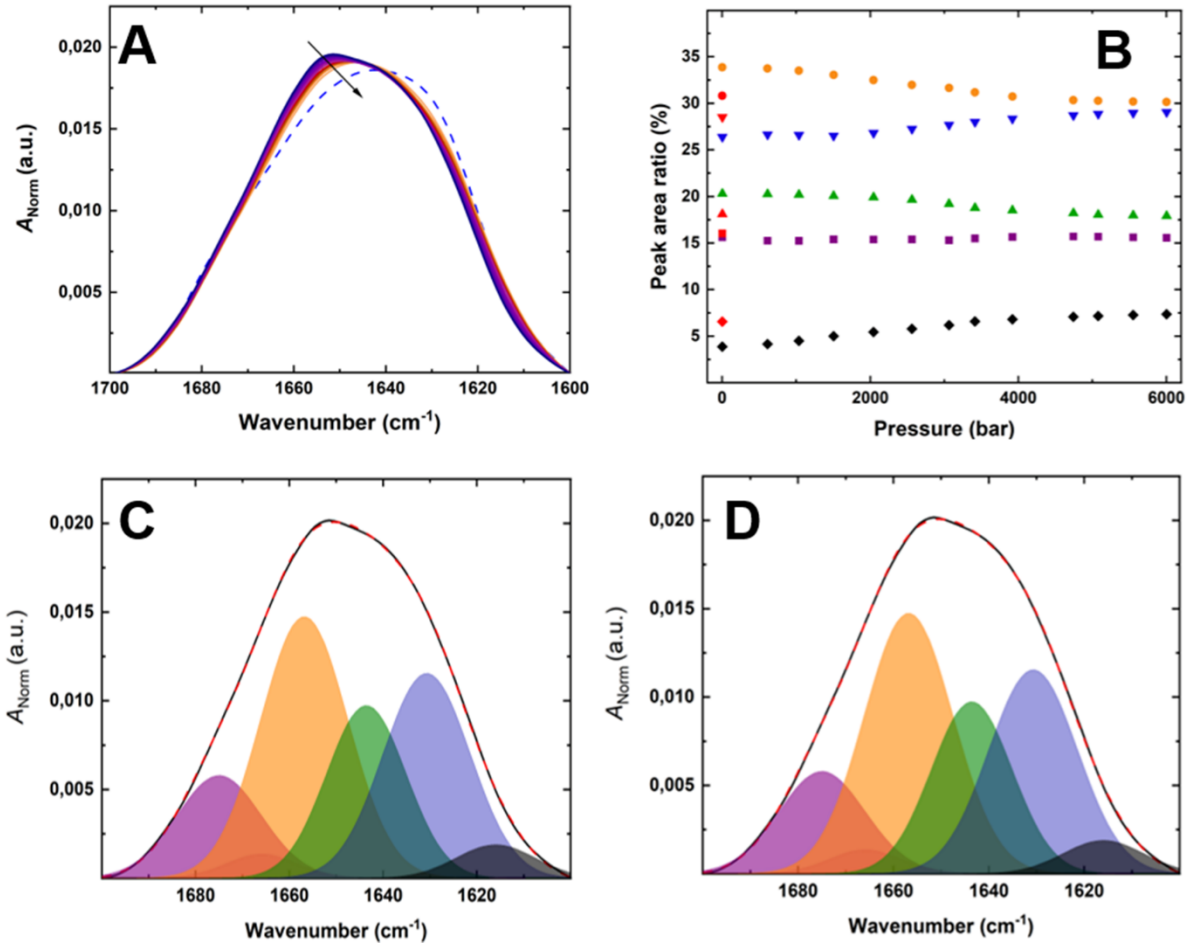

Figure S3. FTIR analysis of Arf6-GDP. A) Amide I' region of the Arf6–GDP FTIR spectrum as a function of pressure in the range of atmospheric pressure bar to 3 kbar. The blue dotted line refers to the protein after returning to atmospheric pressure. B) Pressure dependence of secondary structure content (orange, α-helices at 1657 cm^{-1}, blue, β-sheet at 1631 cm^{-1}, green, random coil at 1644 cm^{-1}, purple, loops at 1665 cm^{-1} and at 1675 cm^{-1} and black, side chains at 1616 cm^{-1}). Red points depressurization to 1 bar. Uncertainty in the peak wavenumber values is ±2 cm^{-1}, and on the pressure, it is ±50 bar. C, D) Deconvolutions of the contribution of secondary structural elements to the overall spectrum at C) 1 bar and D) 3 kbar.

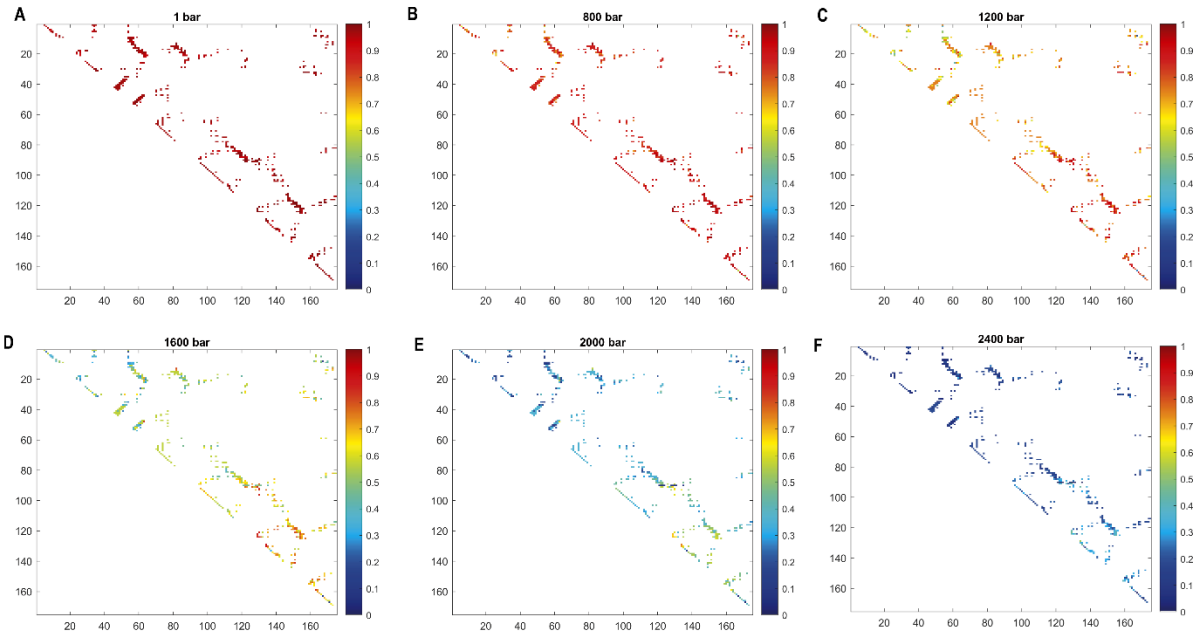

Figure S4. Pressure-dependent fractional contact maps of Arf6-GDP at various pressures. A) 1 bar, B-F) 800 bar and then every 400 bar to 2400 bar. Scales represent the fraction of native contacts of each residue as determined by NMR data.

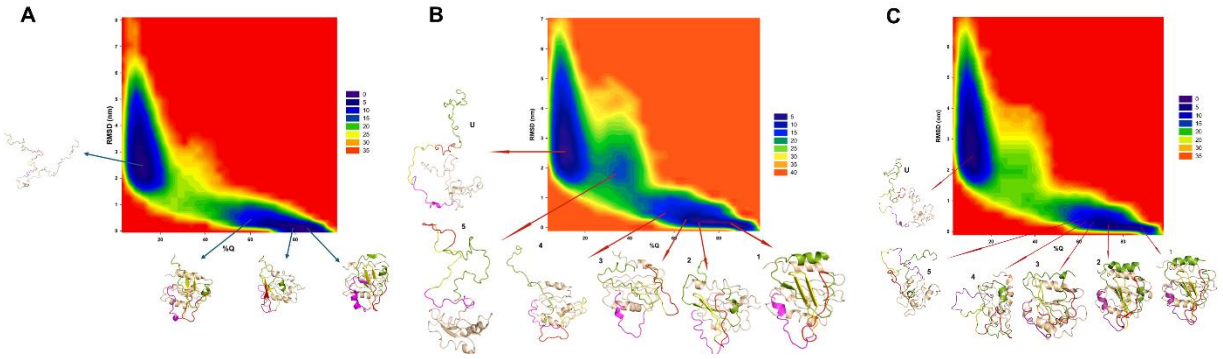

Figure S5. Composite conformational landscape of Arf6-GDP from NMR-constrained Cα coarse grained simulations. RMSD vs percentage of native contacts (%Q) plot along with representative structures shown. Colors according to -ln (N), where dark blue indicates the highest number of configurations, and red the lowest. A) Arf6 FEL calculated from data obtained at pH 6.5, B) Arf1 FEL calculated from data obtained at pH 8.0. C) The broad basin is still apparent for at Q~0.3 for Arf1 at pH 6.5, although it is less stable than at pH 8.5.

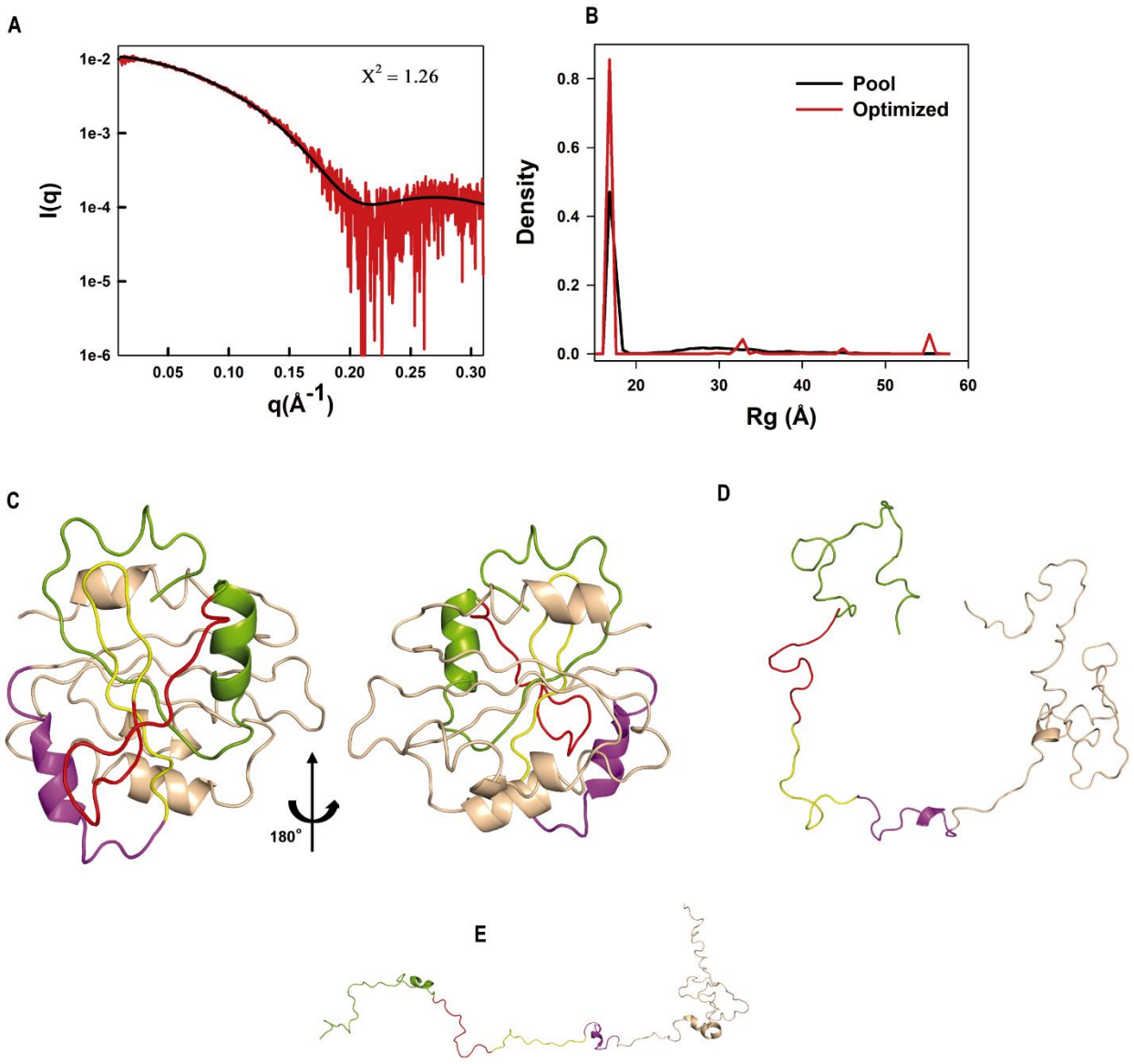

Figure S6. EOM consensus structures of Arf6 at 10 bar. A) Fit of the combined EOM-derived ensemble to experimental SAXS data at 10 bar, with χ^2 showing good agreement with the experimental data. B) Distribution of R_g values for the original pool of structures (black) and the EOM-optimized configurations. C-E) Models obtained by EOM which represent the configurations in the final, optimized ensemble The vast majority represent folded structures as in C – 87%, with a small percentage of partially extended and unfolded structures as in D – 9% and E – 4 %.

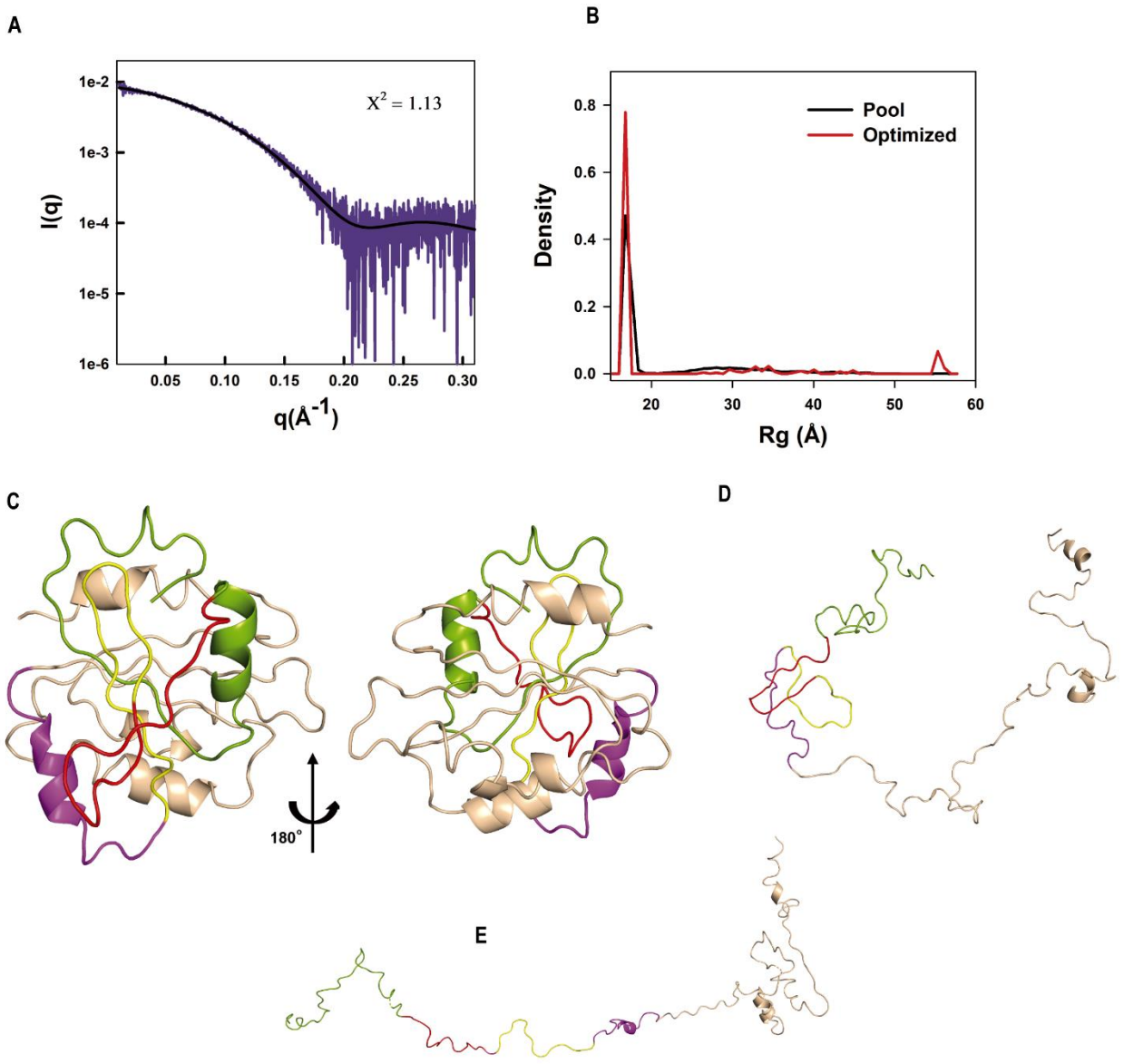

Figure S7. EOM consensus structures at 2000 bar. A) A) Fit of the combined EOM-derived ensemble to experimental SAXS data at 2,000 bar, with χ^2 showing good agreement with the experimental data. B) Distribution of R_g values for the original pool of structures (black) and the EOM-optimized configurations. C-E) Models obtained by EOM which represent the configurations in the final, optimized ensemble. The majority represent folded structures as in C – 79%, with a small percentage of partially extended and unfolded structures as in D – 11% and E – 11%.

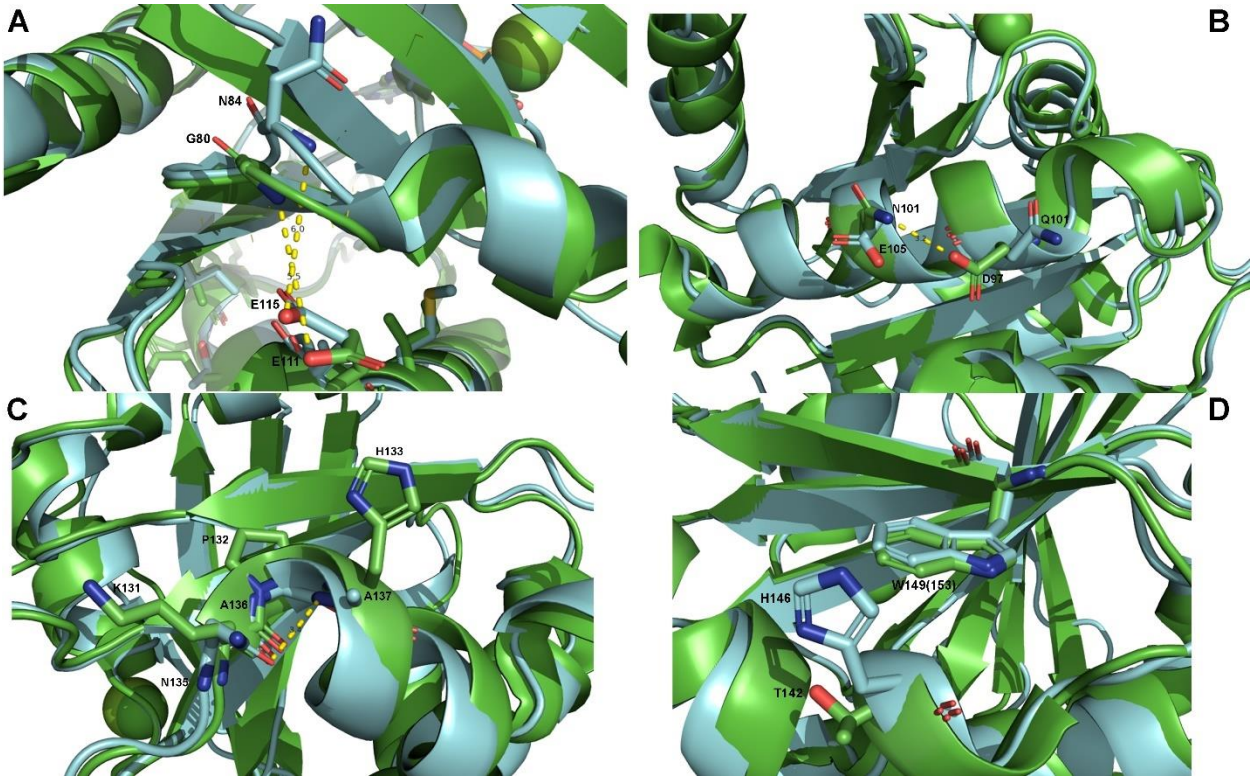

Figure S8. **Substitutions between Arf1 and Arf6 within and outside of the switch region.** A) The mutation of N84 (Arf1, blue) to G80 (Arf6, green) results in a much tighter contact with E111 (115 in Arf1). B) The mutation of N101 and E105 (Arf1, blue) to D97 and Q101 (Arf6, green) results in the formation of a new hydrogen bond which can help explain the increased stability of these residues. C) The mutation of NAA 131-133 (Arf1, blue) to KPH (Arf6, green) results in the bifurcation of a hydrogen bond at the beginning of helix α5 and could explain the decreased stability of these residues. D) The mutation of H146 (Arf1, blue) to T142 (Arf6, green), results in less efficient packing of the residues around the kink of helix α5 with the W residue in the adjacent strand.

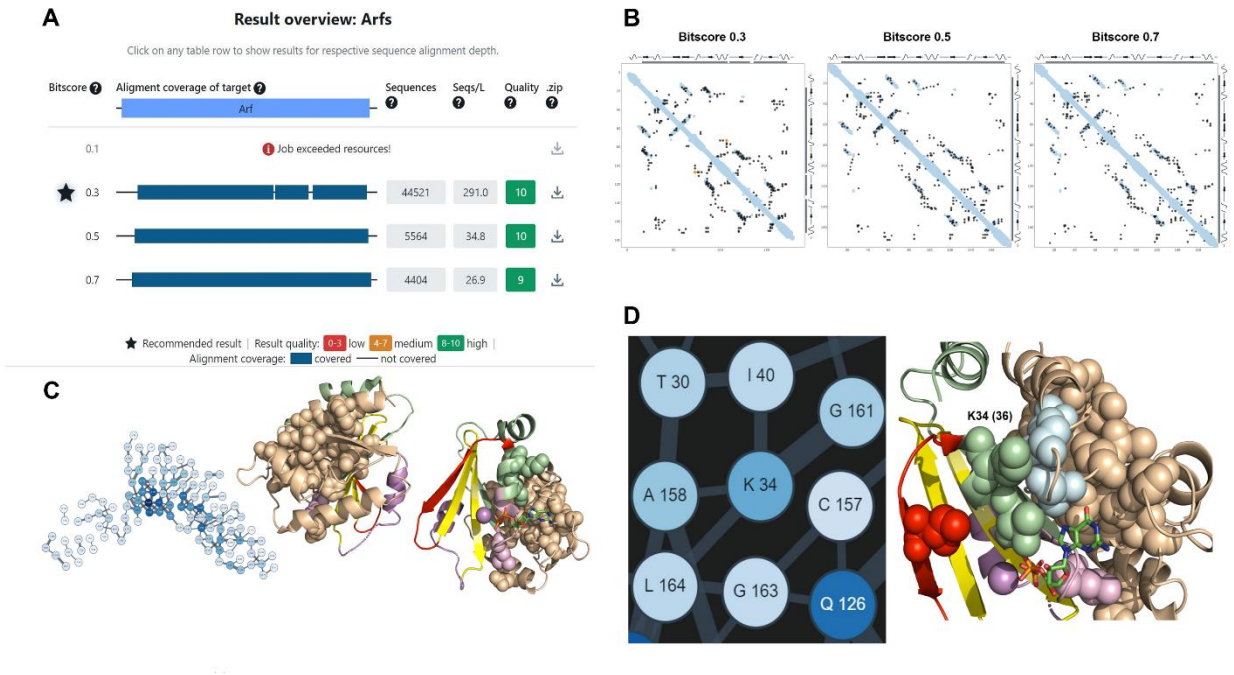

Figure S9. **Evolutionary Coupling analysis of the GTPase family** A) Overall results of the EV Couplings analysis at three different sequence alignment depths. B) Covariance maps for three different Bitscores (sequence alignment depths). C) Visualization of the coupling network. Structures of Arf1 are colored as for Arf6 in Figure 1 in the main text. Coupled residues are shown as spheres. The most highly significant coupling network connects the switch region to the back of the protein.

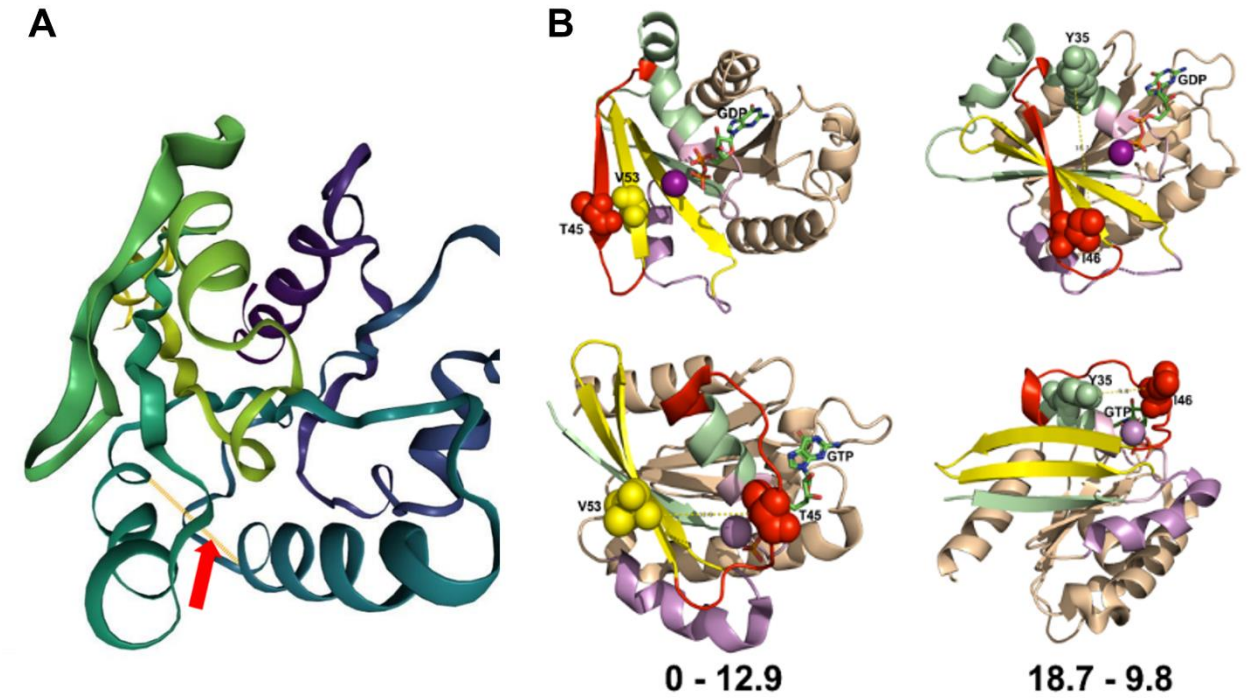

Figure S10. **Structurally distant evolutionary couplings (SDEC)** A) Example of a structurally distant evolutionary coupling (red arrow, yellow line). B, Examples of SDEC due to differences in conformation between GDP and GTP-bound forms of GTPases. Left) Example pf a coupling which involves a direct contact in the GDP-bound form (top), but which is distant in the GTP-bound form (bottom). Right) Example pf a coupling which is distant in the GDP-bound form (top), but which involves closer contact in the GTP-bound form (bottom).

Table S1. Amide backbone assignments for Arf6-GDP.

Res#	Type	N	H	Res#	Type	N	H
2	GLY	109.28	8.43	61	VAL	122.53	9.33
4	VAL	120.0	7.81	63	ASP	116.48	8.64
5	LEU	123.3	8.35	64	VAL	115.08	7.95
6	SER	112.75	8.22	65	GLY	107.52	8.34
7	LYS	120.61	7.31	66	GLY	109.78	8.84
8	ILE	117.95	7.61	67	GLN	118.96	8.62
9	PHE	114.79	7.69	68	ASP	120.57	8.57
10	GLY	106.31	7.82	79	THR	113.99	7.4
12	LYS	122.2	8.12	80	GLY	113.89	8.82
13	GLU	123.83	8.43	81	THR	117.73	8.22
14	MET	122.75	7.85	82	GLN	123.39	8.32
18	MET	124.82	8.84	83	GLY	106	7.73
19	LEU	122.02	8.67	84	LEU	126.86	9.22
20	GLY	102.39	6.33	85	ILE	125.52	9.62
21	LEU	125.23	10.18	86	PHE	130.7	9.71
22	ASP	119.6	8.84	87	VAL	128.8	8.49
23	ALA	123.06	10.82	88	VAL	122.33	8.54
24	ALA	123.15	7.51	89	ASP	123.37	9
25	GLY	101.99	8.6	90	CYS	124.11	8.39
26	LYS	123.22	9.76	91	ALA	122.08	9.14
28	THR	120.01	8.89	92	ASP	120.39	6.92
29	ILE	122.19	8.06	93	ARG	123.7	8.13
30	LEU	117.96	8.09	94	ASP	118.79	8.5
31	TYR	117.75	8.39	95	ARG	114.19	7.19
32	LYS	122.39	8.33	96	ILE	120.97	7.09
33	LEU	116.05	7.63	97	ASP	122.17	8.52
34	LYS	111.84	7.41	98	GLU	122.66	7.78
35	LEU	118.11	8.37	99	ALA	121.94	8.18
36	GLY	103.97	7.44	100	ARG	117.16	8.33
37	GLN	119.83	8.43	101	GLN	117.49	8.16
41	THR	118.11	7.51	102	GLU	117.58	8.43
48	ASN	123.4	7.47	103	LEU	120.23	8.45
50	GLU	127.67	9	106	ILE	119.34	7.69
51	THR	119.88	9.02	107	ILE	109.6	7.95
52	VAL	124.72	8.64	109	ASP	115.35	8.07
53	THR	120.85	8.31	110	ARG	119.06	7.76
54	TYR	127.06	8.97	111	GLU	116.87	9.47
55	LYS	124.55	8.8	112	MET	115.95	7.91
56	ASN	121.52	8.88	113	ARG	120.34	7.21
57	VAL	124.08	9.12	114	ASP	115.22	8.31
58	LYS	126.55	8.24	115	ALA	122.48	7.21
59	PHE	122.65	9.13	117	ILE	121.1	8.39
60	ASN	118.39	8.33	118	LEU	128.44	9.45

Res#	Type	N	H
119	ILE	126.12	9.21
120	PHE	124.96	8.46
121	ALA	130.46	8.76
122	ASN	124.55	8.53
123	LYS	114.02	7.33
124	GLN	112.2	8.1
125	ASP	114.08	9.77
126	LEU	122.38	7.44
128	ASP	115.76	8.67
129	ALA	121.36	7.44
130	MET	122.21	8.57
131	LYS	121.56	8.91
133	HIS	114.12	8.51
134	GLU	121.25	6.89
135	ILE	119.36	7.9
136	GLN	118.09	8.32
137	GLU	117.29	7.05
138	LYS	120	8.87
139	LEU	113.05	8.18
140	GLY	108.02	7.8
141	LEU	116.31	7.39
142	THR	107.15	7.4
143	ARG	116.35	7.24
144	ILE	121.41	7.87
145	ARG	125.51	8.7
146	ASP	117.55	8.72
147	ARG	115.5	7.39
148	ASN	121	8.85
149	TRP	119.56	7.69
150	TYR	120.41	8.03
151	VAL	126.03	7.94
152	GLN	127.71	9.14
154	SER	118.23	8.84
155	CYS	120.2	8.55
156	ALA	132.45	9.43
157	THR	102.64	7.07
158	SER	115.35	7.61
159	GLY	112.34	8.38
160	ASP	124.78	7.96
161	GLY	112.92	8.81
162	LEU	117.68	7.39
163	TYR	119.25	8.87
164	GLU	124.81	10.31
165	GLY	108	8.6
166	LEU	120.57	8.41
167	THR	118.46	8.51
168	TRP	124.28	7.68
169	LEU	120.29	8.25
170	THR	108.79	8.18
171	SER	115.51	7.79
172	ASN	116.23	7
173	TYR	121.54	7.32
174	LYS	127.24	8.54
175	SER	124.11	7.84

Table S2. ΔG_{ex} and ΔV_{ex} values for Arf6-GDP.

Res #	ΔGex	σΔG	ΔVex	σΔV	Res #	ΔGex	σΔG	ΔVex	σΔV
2	0.88	0.13	51.29	7.34	61	1.41	0.12	57.35	5.41
4	1.35	0.10	44.74	3.59	64	1.84	0.20	58.93	8.62
5	1.76	0.18	57.82	7.59	65	1.82	0.08	46.00	2.49
6	1.79	0.10	52.08	3.16	66	1.33	0.08	45.01	3.07
8	2.27	0.16	67.41	6.02	67	1.39	0.14	32.44	4.50
9	1.59	0.18	52.75	7.53	68	1.17	0.09	46.88	3.74
10	2.59	0.11	75.39	3.92	79	1.63	0.12	44.81	4.02
12	1.44	0.08	43.67	2.87	80	2.44	0.15	73.79	5.73
14	3.87	0.26	86.66	9.51	81	2.17	0.24	62.77	10.29
18	2.76	0.22	81.23	9.12	82	2.89	0.29	58.65	10.36
19	2.23	0.18	58.13	6.33	83	3.21	0.16	72.96	5.01
20	1.29	0.19	58.59	11.18	84	1.21	0.10	38.12	3.69
21	1.39	0.16	36.80	5.92	85	2.14	0.12	61.57	4.28
22	1.25	0.07	49.31	2.94	86	2.19	0.18	49.90	5.81
23	2.53	0.20	68.24	7.63	87	3.25	0.17	81.29	5.57
24	1.64	0.06	48.18	2.06	88	1.22	0.10	30.31	3.11
25	1.69	0.12	51.51	4.52	89	2.39	0.18	53.61	5.65
26	1.31	0.17	51.66	8.25	91	2.72	0.23	54.36	7.31
28	2.07	0.17	50.36	5.59	92	2.42	0.15	50.90	4.30
29	1.69	0.16	46.19	5.58	93	2.38	0.16	47.52	4.73
30	3.91	0.38	87.46	17.50	94	2.80	0.19	61.26	5.92
31	2.49	0.18	63.25	6.15	95	1.93	0.09	45.24	2.62
32	3.71	0.50	89.63	31.97	96	3.35	0.19	71.13	5.69
33	1.51	0.07	53.11	2.67	97	1.77	0.13	41.09	3.97
35	2.29	0.16	72.05	6.48	98	3.02	0.12	62.64	3.20
36	2.75	0.29	102.82	18.42	99	2.81	0.23	62.50	7.91
37	1.66	0.11	55.71	4.04	100	2.79	0.17	63.64	5.51
41	1.56	0.12	60.48	5.13	101	3.29	0.29	64.94	10.47
48	3.64	0.22	76.93	6.85	102	2.83	0.22	64.83	7.68
50	2.56	0.17	80.90	6.91	103	1.77	0.10	44.83	2.97
51	2.12	0.18	68.23	7.50	106	1.28	0.11	34.09	3.70
52	2.35	0.21	54.41	7.40	107	2.73	0.17	71.58	5.93
53	2.27	0.07	63.06	2.31	109	1.86	0.11	41.24	3.16
54	1.81	0.10	67.89	4.36	110	2.95	0.20	67.12	6.36
55	2.59	0.21	86.00	10.17	111	1.85	0.12	55.28	4.28
56	1.89	0.11	61.21	4.24	112	2.09	0.15	52.75	4.84
57	1.65	0.14	58.31	6.05	114	1.90	0.07	51.61	2.18
58	2.75	0.25	63.78	9.39	115	1.65	0.07	45.69	2.18
59	3.54	0.28	88.20	11.53	117	2.91	0.33	61.43	13.32
60	1.71	0.14	51.85	5.41	118	3.55	0.25	77.71	8.61

Res #	ΔGex	σΔG	ΔVex	σΔV	Res #	ΔGex	σΔG	ΔVex	σΔV
119	3.95	0.25	80.64	8.30	163	3.74	0.36	65.02	14.03
120	2.09	0.19	54.08	6.63	164	3.38	0.20	73.83	6.45
121	3.49	0.28	74.01	10.26	165	2.77	0.14	57.69	3.96
122	3.16	0.23	62.19	7.31	166	2.98	0.31	70.07	13.24
123	2.04	0.14	40.56	4.16	168	3.07	0.26	68.58	9.72
124	3.40	0.32	66.78	11.83	169	2.33	0.13	54.77	3.90
125	2.23	0.12	41.16	3.15	170	2.02	0.13	52.41	4.07
126	3.09	0.25	55.76	8.03	171	1.66	0.13	38.96	4.13
128	2.05	0.15	41.84	4.63	172	2.00	0.15	48.83	4.72
129	4.72	0.40	82.01	15.97	173	2.28	0.17	51.28	5.51
131	2.07	0.13	34.93	3.52	174	1.74	0.20	50.69	7.88
133	1.50	0.24	70.64	15.86	175	1.76	0.11	49.05	3.47
134	2.59	0.21	44.62	6.47					
135	1.63	0.09	33.84	2.53					
136	1.75	0.12	33.87	3.51					
137	2.13	0.09	41.13	2.38					
138	1.13	0.09	27.82	3.02					
139	3.04	0.19	63.41	5.74					
140	3.91	0.20	81.46	6.21					
141	3.70	0.33	75.95	13.13					
142	1.41	0.06	36.87	1.70					
143	1.85	0.09	37.24	2.54					
144	1.42	0.08	39.84	2.60					
145	1.15	0.09	35.57	3.17					
146	1.65	0.09	39.80	2.52					
147	4.26	0.47	88.49	24.59					
148	2.00	0.08	40.78	2.10					
149	1.88	0.12	38.47	3.60					
150	2.17	0.14	44.45	3.88					
151	4.29	0.27	86.27	9.34					
152	3.36	0.25	66.37	7.99					
154	3.19	0.28	63.18	9.61					
155	1.50	0.11	29.81	3.09					
156	2.92	0.17	61.77	4.96					
157	3.53	0.20	74.33	6.07					
158	2.19	0.17	35.01	4.85					
159	2.55	0.14	50.21	3.98					
160	2.62	0.23	56.25	7.69					
161	2.48	0.16	48.59	4.47					
162	2.14	0.12	51.38	3.78					

Table S3. Results of EOM modeling of Arf6-GDP configurations

Pressure	Model #	Fraction	R_g (Å)	D_{max} (Å)
10 bar	1	0.87	16.90	50.20
	2	0.09	33.10	87.60
	3	0.04	55.80	180.40
2000 bar	1	0.79	16.90	50.20
	2	0.11	34.60	95.90
	3	0.11	56.10	181.60

Table S4. Difference in local stability between residues in Arf6 and Arf1
*residues from helices α4 and α5 are highlighted in grey.

Arf6 Res	Equivalent Res # in Arf1	ΔΔG	Arf6 Res	Equivalent Res # in Arf1	ΔΔG	Arf6 Res	Equivalent Res # in Arf1	ΔΔG
6	10	-0.05	80	84	1.45	131	135	-1.91
10	14	1.39	81	85	0.15	133	137	-0.93
12	16	-0.40	82	86	-0.36	134	138	-0.78
14	18	2.40	83	87	1.63	135	139	-2.29
19	23	0.82	84	88	-1.43	136	140	-0.19
20	24	-0.68	85	89	-0.05	137	141	0.07
21	25	0.01	86	90	0.82	138	142	-1.41
22	26	-0.15	87	91	1.02	139	143	-0.34
23	27	-1.32	88	92	-2.39	140	144	1.12
25	29	-0.17	89	93	-0.14	141	145	1.24
28	32	0.79	91	95	0.02	142	146	-1.20
29	33	-0.08	92	96	0.67	143	147	-0.66
30	34	2.09	93	97	0.86	144	148	-0.24
31	35	0.07	94	98	1.11	145	149	-0.59
32	36	1.51	95	99	0.16	147	151	2.74
33	37	-0.44	96	100	1.59	148	152	-1.29
35	39	0.74	98	102	-1.12	149	153	-2.30
36	40	1.57	99	103	0.83	150	154	0.75
37	41	-0.53	100	104	0.02	151	155	1.87
41	45	-0.18	101	105	1.06	152	156	1.65
48	52	1.80	102	106	0.58	154	158	0.25
50	54	0.60	103	107	-1.69	155	159	-0.15
51	55	0.06	106	110	-1.51	156	160	-0.63
52	56	1.60	107	111	-0.26	157	161	0.75
53	57	0.00	109	113	-1.73	158	162	0.95
54	58	-0.30	114	118	-0.50	159	163	-0.17
55	59	0.92	115	119	-1.03	160	164	0.59
56	60	0.00	117	121	0.18	162	166	-1.32
57	61	0.03	120	124	-3.05	163	167	1.13
59	63	1.91	121	125	0.76	164	168	0.44
61	65	-0.55	122	126	1.03	165	169	0.55
64	68	0.48	123	127	0.77	166	170	1.50
65	69	0.80	124	128	0.23	168	172	0.48
66	70	-0.11	125	129	0.87	169	173	0.28
67	71	-0.41	126	130	1.11	172	176	-0.03
68	72	-0.09	128	132	0.69	175	179	0.25
79	83	0.52	129	133	3.06			

Table S5. Amide backbone assignments for Arf6α5-GDP.

Res#	N	H	Res#	N	H	Res#	N	H
2	109.61	8.46	66	109.90	8.75	129	121.27	7.35
4	120.15	7.77	67	118.85	8.54	130	123.52	8.49
6	112.60	8.15	68	120.44	8.47	131	119.48	8.64
7	120.50	7.21	79	114.05	7.31	132	118.37	8.77
8	117.98	7.53	80	113.84	8.74	133	124.03	8.28
9	114.40	7.56	81	117.65	8.17	134	121.56	8.42
10	106.08	7.70	83	106.10	7.66	135	118.65	8.54
12	122.10	8.05	84	127.01	9.15	136	117.83	7.91
13	123.65	8.33	85	125.48	9.53	137	119.92	7.30
14	122.88	7.76	86	130.65	9.62	139	113.64	8.15
18	124.96	8.73	87	128.71	8.37	140	108.59	7.82
19	121.94	8.59	88	122.23	8.46	141	116.22	7.12
20	102.44	6.24	89	123.38	8.89	142	113.32	8.08
21	125.23	10.12	91	122.10	9.05	143	111.77	7.37
22	119.58	8.75	92	120.44	6.84	144	123.44	7.69
23	123.00	10.71	93	123.56	8.07	145	125.48	8.55
24	123.15	7.40	94	118.72	8.41	146	117.53	8.67
25	101.91	8.50	95	114.36	7.11	147	115.72	7.41
26	123.20	9.65	96	120.85	7.00	148	120.73	8.72
28	119.97	8.80	97	122.20	8.44	149	119.49	7.66
29	122.15	7.97	98	122.57	7.70	150	120.55	7.98
30	117.93	8.02	99	121.98	8.07	151	126.27	7.69
31	117.71	8.32	100	117.19	8.29	152	127.17	9.06
32	122.38	8.20	101	117.23	8.07	154	119.95	8.89
33	115.93	7.52	102	117.58	8.31	155	120.17	8.52
34	111.78	7.32	103	120.25	8.35	156	132.53	9.35
35	118.54	8.33	106	119.16	7.64	157	102.86	7.02
36	104.12	7.36	107	109.91	7.80	158	115.49	7.55
37	120.01	8.35	109	114.97	7.95	159	112.27	8.30
41	118.09	7.41	110	119.17	7.69	160	124.89	7.89
48	123.25	7.39	111	116.96	9.41	161	112.98	8.75
50	127.58	8.90	112	116.07	7.82	162	117.64	7.33
51	119.92	8.92	113	120.15	7.12	163	119.20	8.80
52	124.72	8.54	114	115.29	8.19	164	124.75	10.27
53	120.88	8.22	115	122.51	7.14	165	107.84	8.53
54	127.11	8.87	117	121.33	8.32	166	120.62	8.34
55	124.58	8.71	118	128.35	9.34	167	118.55	8.41
56	121.56	8.81	119	126.29	9.11	168	124.23	7.56
57	124.09	9.05	120	124.97	8.39	169	120.36	8.15
58	126.53	8.17	121	130.68	8.49	170	108.55	8.07
59	122.63	9.03	122	124.75	8.49	171	115.29	7.66
60	118.29	8.23	123	113.66	7.22	172	116.16	6.90
61	122.51	9.24	124	112.33	7.99	173	121.36	7.22

63	116.52	8.56	125	113.74	9.67	174	126.95	8.52
64	115.20	7.87	126	122.37	7.37	175	124.27	7.75
65	107.51	8.25	128	115.86	8.59			

Table S6. Differences in stability between WT Arf6-GDP and Arf6α5-GDP.

Res #	WT ΔGapp	α5 ΔGapp	ΔΔG	Res #	WT ΔGapp	α5 ΔGapp	ΔΔG
2	0.88	1.14	0.26	80	2.44	2.08	-0.36
4	1.35	1.43	0.08	81	2.17	1.74	-0.43
6	1.79	1.65	-0.14	83	3.21	1.66	-1.55
8	2.27	1.64	-0.63	84	1.21	2.16	0.95
9	1.59	1.75	0.16	85	2.14	2.35	0.21
10	2.59	2.27	-0.32	86	2.19	5.57	3.37
12	1.44	2.01	0.57	87	3.25	2.46	-0.79
14	3.87	3.14	-0.73	89	2.39	1.98	-0.41
18	2.76	2.89	0.12	91	2.72	3.49	0.77
19	2.23	2.55	0.32	92	2.42	1.58	-0.84
20	1.29	1.89	0.60	93	2.38	2.26	-0.12
22	1.25	1.66	0.41	94	2.80	3.62	0.82
23	2.53	1.95	-0.58	95	1.93	2.05	0.12
24	1.64	2.89	1.25	96	3.35	2.71	-0.64
25	1.69	1.67	-0.01	97	1.77	1.74	-0.03
26	1.31	1.43	0.12	98	3.02	4.18	1.17
29	1.69	2.60	0.91	99	2.81	3.54	0.73
30	3.91	3.63	-0.28	100	2.79	4.49	1.71
31	2.49	2.59	0.11	101	3.29	1.56	-1.73
32	3.71	1.94	-1.76	102	2.83	1.45	-1.38
33	1.51	3.76	2.25	103	1.77	4.93	3.17
36	2.75	1.44	-1.31	106	1.28	1.88	0.60
41	1.56	2.22	0.66	107	2.73	1.89	-0.84
48	3.64	2.94	-0.70	109	1.86	4.58	2.72
50	2.56	2.06	-0.50	110	2.95	2.83	-0.13
51	2.12	1.83	-0.29	111	1.85	2.11	0.26
53	2.27	1.63	-0.64	112	2.09	2.56	0.47
54	1.81	1.73	-0.08	114	1.90	1.66	-0.24
55	2.59	1.50	-1.09	115	1.65	1.70	0.05
56	1.89	2.79	0.90	118	3.55	3.16	-0.39
57	1.65	2.99	1.34	119	3.95	4.30	0.35
58	2.75	3.77	1.02	120	2.09	2.67	0.58
59	3.54	5.93	2.39	121	3.49	3.29	-0.19
61	1.41	1.88	0.47	122	3.16	1.28	-1.88
64	1.84	3.99	2.16	123	2.04	2.10	0.06
65	1.82	2.29	0.46	124	3.40	2.98	-0.42
66	1.33	1.40	0.07	125	2.23	2.34	0.11
67	1.39	1.40	0.02	126	3.09	2.36	-0.72
68	1.17	1.47	0.30	128	2.05	4.95	2.90
79	1.63	2.41	0.78	129	4.72	4.27	-0.45

Res #	WT ΔGapp	α5 ΔGapp	ΔΔG
133	1.50	1.72	0.22
134	2.59	4.35	1.76
135	1.63	5.83	4.20
136	1.75	2.09	0.34
137	2.13	2.16	0.03
140	3.91	3.23	-0.68
141	3.70	3.26	-0.44
143	1.85	3.33	1.48
144	1.42	1.45	0.03
145	1.15	1.36	0.21
146	1.65	1.82	0.17
147	4.26	3.92	-0.34
148	2.00	2.93	0.93
149	1.88	2.07	0.20
150	2.17	3.37	1.20
151	4.29	3.05	-1.24
152	3.36	2.64	-0.73
154	3.19	1.65	-1.53
155	1.50	3.79	2.30
156	2.92	2.75	-0.17
157	3.53	2.54	-0.99
158	2.19	3.85	1.66
159	2.55	2.84	0.28
160	2.62	2.13	-0.49
161	2.48	2.15	-0.33
162	2.14	1.39	-0.74
163	3.74	0.95	-2.78
164	3.38	2.67	-0.71
165	2.77	2.21	-0.56
166	2.98	0.70	-2.28
169	2.33	2.42	0.09
170	2.02	2.26	0.24
171	1.66	1.68	0.03
172	2.00	1.44	-0.55
173	2.28	2.89	0.61
174	1.74	2.97	1.24
175	1.76	3.02	1.26

Table S7. FPECs in Arf1 and Arf6.

FPECs from Bitscore 0.3 where confidence was over 94% as well as where distance between residues in the GDP-bound structure was 9 or more angstroms. Residues marked with an asterisk are shared FPECs between Arf1 and Arf6. D_GDP and D_GTP indicate the distance (Å) between residue pairs in the structure.

Arf6						**Arf1**				
R1	**R2**	**%conf**	**D_GDP**	**D_GTP**		**R1**	**R2**	**%conf**	**D_GDP**	**D_GTP**
P127	H133	0.99	14.7	12.2		R97	L143	100	11.2	12.1
E137*	P153*	0.99	12	12.6		R104*	H150*	99.6	17.8	16.2
R100*	D146*	0.99	13.5	17.3		D141*	A157*	99.4	14.1	14
P127*	P153*	0.97	13.6	13.3		V100	S147	97.7	14.2	13.7
L139	R145	0.95	10.6	13.9		A112	L121	97.4	11.7	11.2
L139	D146	0.94	11.1	11.1		L148	I145	96.8	10	9.8
						P131*	A157*	95.5	12.6	12.9
						P131	E138	95.4	9	9.7
						G144	H150	95.1	11.4	13.2